A Statistical Comparison Between Proton Microinstabilities and Nonlinear Effects in Space Plasmas

Ramiz A. Qudsi[1],
Bennett A. Maruca[1,2], R. Bandyopadhyay[1], A. Chasapis[1], S. P. Gary[3],
R. Chhiber[1], T. N. Parashar[1], W. H. Matthaeus[1,2], J. L. Burch[4],
T. E. Moore[5], C. J. Pollock[6], B. J. Giles[5], W. R. Paterson[5], J. Dorelli[5],
D. J. Gershman[5], R. B. Torbert[6], & R. J. Strangeway[8]

[1]Univ. Delaware [2]Bartol Res. Inst. [3]Space Sci. Inst. [4]Southwest Res. Inst.
[5]NASA/GSFC [6]Denali Sci. [7]Univ. New Hampshire [8]Univ. California, LA

ahmadr@udel.edu

10 October 2019

Introduction:
Microphysics of Space-Plasma Ions

Velocity Distribution Function (VDF)

- Probability distribution of particle velocities (for a given species, j)
- Relation of VDF moments to bulk parameters
- In local thermal equilibrium (LTE), all particle species have
  - . . . the same temperature.
  - . . . the same bulk velocity.
  - . . . Maxwellian VDF's.
- VDFs of space-plasma ions
  - Highly variable
  - Frequently exhibit departures from LTE
    - Preserved by low rates of collisions among ions
    - Reveal the plasma's "history"

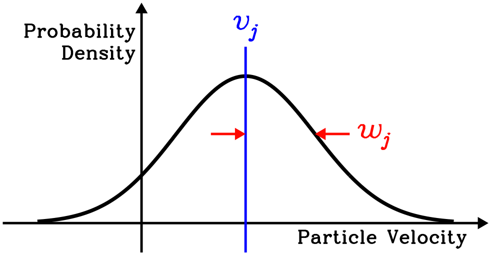

Bulk Parameters:

n_j – particle density (0^{th} moment)
v_j – bulk velocity (1^{st} moment)
w_j – thermal speed
T_j – temperature (2^{nd} moment)

$$k_B\,T_j = m_j\,w_j^2\,/\,2$$

Exemplar VDF for Protons

- 2-D projection of 3-D VDF
- Contours of phase-space density
- Overlaid axis of magnetic-field
- Multiple departures from LTE
- Temperature anisotropy
  - Elongation/compression of contours
  - Alignment with magnetic field: $T_{\perp j}$ and $T_{\parallel j}$
  - Anisotropy ratio: $R_j = T_{\perp j} \,/\, T_{\parallel j}$

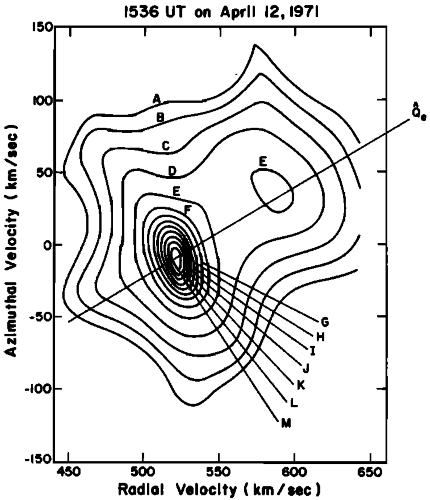

Feldman et al. (*JGR*, 1973); *IMP-6*

Exemplar VDF for Protons

- Global and local processes affecting plasma
  - Expansion:
    Large-scale trends in fluid moments
  - Shocks:
    Discontinuities in fluid moments
  - Turbulence:
    Spectra of fluctuations
  - Coulomb collisions:
    Soft scattering of individual particles
  - Microinstabilities:
    Limits on departures from LTE

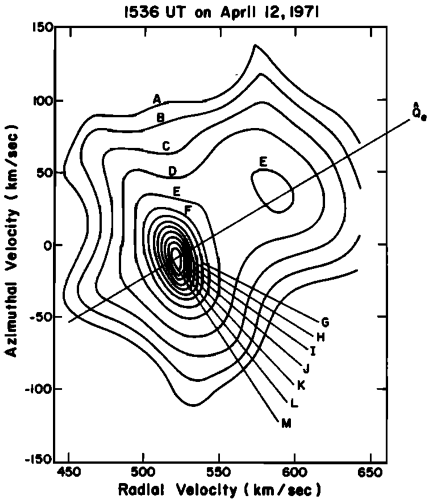

Feldman et al. (*JGR*, 1973); *IMP-6*

Overview

Questions:

- How are the microinstabilities distributed in the space-plasma?
- How do microinstabilities regulate temperature anisotropy in the magnetosheath?
- Where and when does this regulation occur?
- Are the linear time scales even important?

Outline:

- Kinetic theory of temperature-anisotropy instabilities
- Instabilities in PIC simulation: regulation of temperature anisotropy
- Temperature anisotropy instabilities in Earth's magnetosheath and solar wind
- Interplay of turbulence and instabilities

Kinetic Theory of Temperature-Anisotropy Instabilities

Linear Vlasov Theory of Instabilities

- VDF $f_j(t, \mathbf{r}, \mathbf{u})$ for ion species j
  - t = time; $\mathbf{r}$ = position; $\mathbf{u}$ = velocity
- Vlasov equation: collisionless Boltzmann equation

$$\frac{df}{dt} = \frac{\partial f_j}{\partial t} + \mathbf{u} \cdot \frac{\partial f_j}{\partial \mathbf{r}} + \frac{q_j}{m_j} (\mathbf{E} + \mathbf{u} \times \mathbf{B}) \cdot \frac{\partial f_j}{\partial \mathbf{u}} = 0$$

- Analysis of microinstabilities:
  - Assume homogeneous background
  - Impose small-amplitude perturbation $\propto e^{i(\mathbf{k}\cdot\mathbf{r} - \omega\, t)}$
    - $\mathbf{k}$ = wave vector
    - ω = frequency (complex)
    - $\omega = \omega_r + i\,\gamma$
  - Expand Vlasov and Maxwell's equations to first order
  - Solve for dispersion relation: ω as a function of $\mathbf{k}$

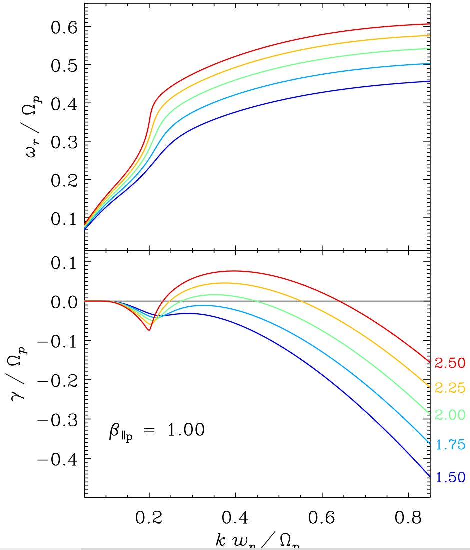

Linear Vlasov Theory of Instabilities

- Exemplar dispersion curves
  - Plot of $\omega = \omega_r + i\,\gamma$ as function of k
  - Proton cyclotron instability
  - Color: different values of $R_p = T_{\perp p} \,/\, T_{\parallel p}$
- Growth rate of mode: $\gamma = \gamma(\mathbf{k})$
  - $\gamma < 0$: decreasing amplitude (damped wave)
  - $\gamma > 0$: increasing amplitude (instability)
- Instability growth rate: $\gamma_{\max} = \max_{\forall \mathbf{k}} \gamma$
  - $\gamma_{\max} = 0$: plasma stable (all modes damped)
  - $\gamma_{\max} > 0$: plasma unstable (growing modes)

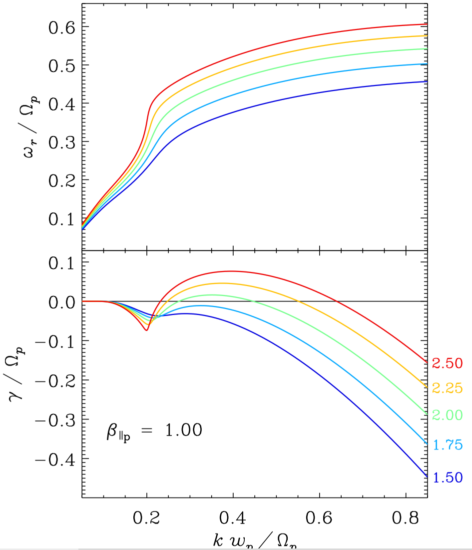

Ion Temperature-Anisotropy Instabilities

	Parallel ($\mathbf{k} \parallel \mathbf{B}$) & Propagating ($\omega_\mathrm{r} > 0$)	Oblique ($\mathbf{k} \nparallel \mathbf{B}$) & Non-Prop. ($\omega_\mathrm{r} = 0$)
$T_{\perp j} > T_{\parallel j}$ ($R_j > 1$)	Ion-cyclotron (Alfven mode)	Mirror (kinetic slow mode)
$T_{\perp j} < T_{\parallel j}$ ($R_j < 1$)	Parallel firehose (fast/whistler mode)	Oblique firehose (Alfven mode)

- Instabilities driven by $R_j \neq 1$
- Separate modes for $R_j > 1$ and < 1
- Separate modes for **k** parallel and oblique to **B**
- Value of γ strongly dependent on R_j and plasma beta:

$$\beta_{\parallel j} \equiv \frac{n_j \, k_\mathrm{B} \, T_{\parallel j}}{B^2 \, / \, (2 \, \mu_0)}$$

- Example: $\gamma_\mathrm{max}(\beta_{\parallel p}, R_p)$ for mirror instability

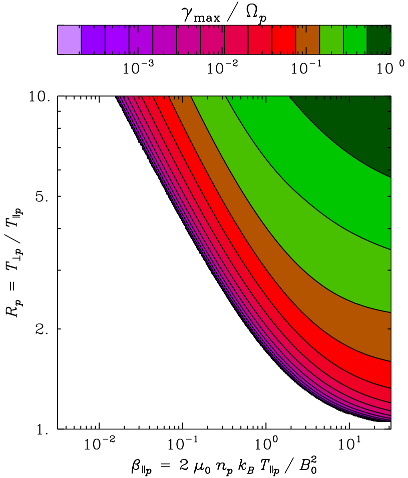

Maruca (PhD thesis, 2012)

Instability Regulation of Temperature Anisotropy

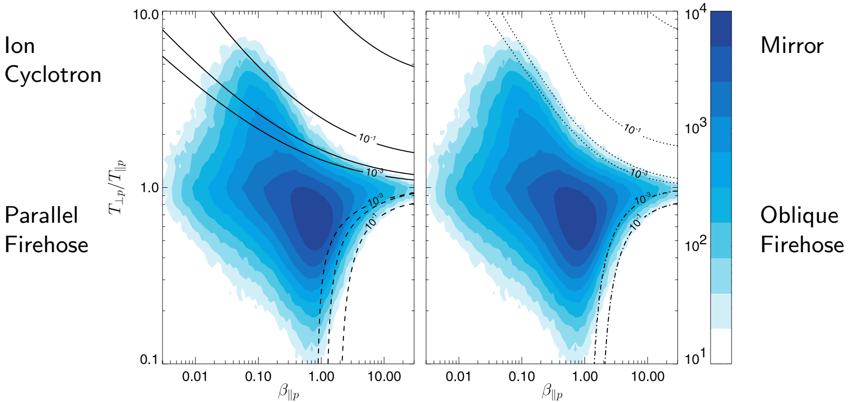

- Joint distributions of $(\beta_{\parallel j}, R_j)$-data
  - Essentially, 2-D histograms
  - "Brazil plots"
- Popularized by Hellinger et al. (*GRL*, 2006)
  - Proton measurements *Wind*/SWE
  - Data bins smoothed into curves
  - Overlaid: contours of constant γ (theory)

Instability Regulation of Temperature Anisotropy

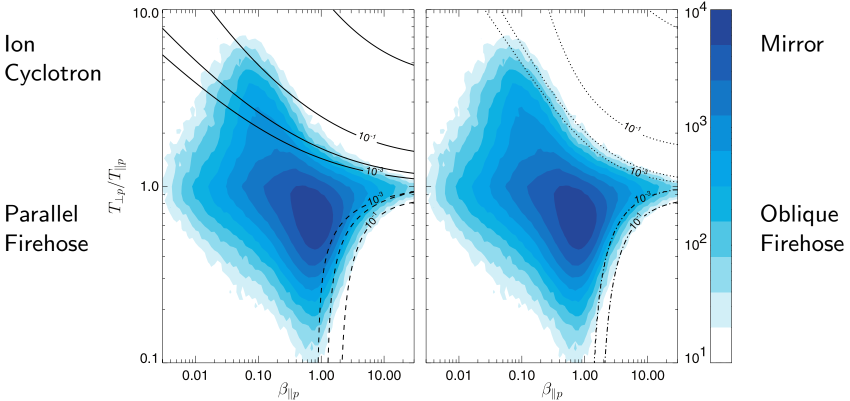

- Alignment of data with γ contours
  - Excellent for oblique modes (right)
  - Worse for parallel modes (left) – despite theoretically stricter limits (especially at low-$\beta_{\parallel p}$)
  - Cause unknown; possibly due to differences in propagation

Instabilities and Heating

- Probability density of $(\beta_{\parallel p}, R_p)$
  - Counts normalized by bin size
  - Bins smoothed into contours
- Temperature T_p over $(\beta_{\parallel p}, R_p)$-plane
  - Temperature enhancement in marginally unstable plasma
  - Heating (versus cooling) produces temperature anisotropy that drives instabilities
- Temperature components $T_{\perp p}$ and $T_{\parallel p}$
  - Enhancements in both at respective instability thresholds
  - Strongly preferential heating
  - No indications of cooling driving instabilities

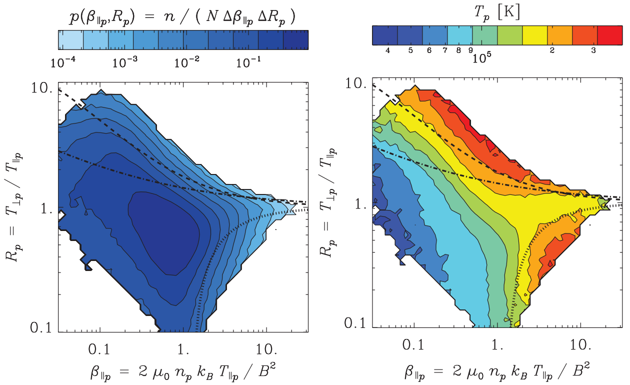

Maruca et al. (*PRL*, 2011)

Instabilities and Heating

- Probability density of $(\beta_{\|p}, R_p)$
  - Counts normalized by bin size
  - Bins smoothed into contours
- Temperature T_p over $(\beta_{\|p}, R_p)$-plane
  - Temperature enhancement in marginally unstable plasma
  - Heating (versus cooling) produces temperature anisotropy that drives instabilities
- Temperature components $T_{\perp p}$ and $T_{\|p}$
  - Enhancements in both at respective instability thresholds
  - Strongly preferential heating
  - No indications of cooling driving instabilities

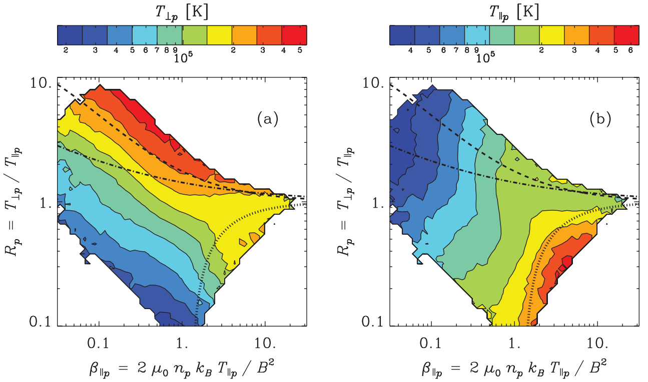

Maruca et al. (*PRL*, 2011)

Instabilities and Magnetic Structures

- Magnetic fluctuations over $(\beta_{\parallel p}, R_p)$-plane
  - Enhanced near thresholds
  - Compressive near mirror threshold
- Magnetic PVI over $(\beta_{\parallel p}, R_p)$-plane
  - Indicator of magnetic structure (turbulence)
  - Enhanced near thresholds
- Development of microinstabilities in turbulent plasma

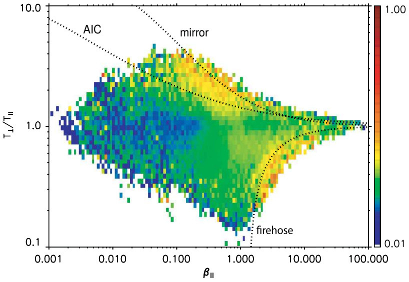

Bale et al. (*PRL*, 2009)

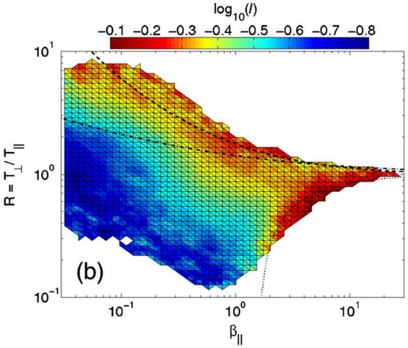

Osman et al. (*PRL*, 2012)

Temperature Anisotropy Instabilities in PIC simulation and Earth's Magnetosheath

Instability Analysis of PIC Simulation

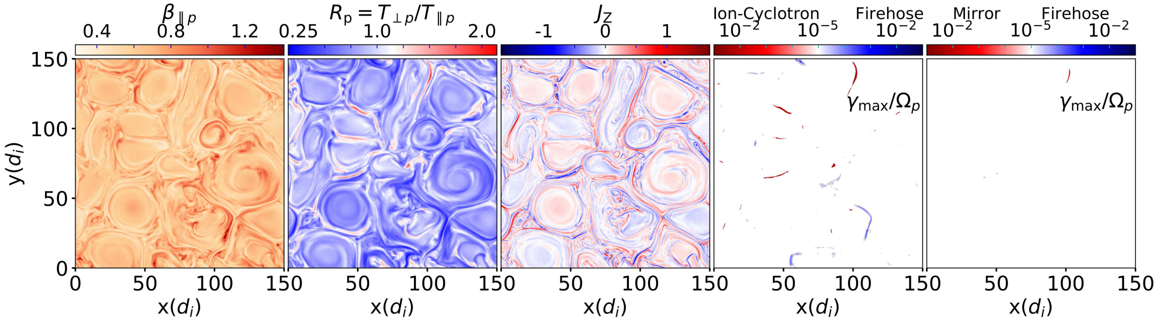

Qudsi et al. (*ApJ*, submitted)

- 2.5-D fully kinetic PIC simulation
- Departures from LTE near current sheets (Greco et al., *PRL*, 2008; *PhRvE*, 2012)
- Linear Vlasov theory: growth rates of $R_p \neq 1$ instabilities
- Distinct regions of $\gamma_{\text{max}} > 0$
  - More with parallel than oblique instabilities
  - Near (not co-local with) current sheets
- Turbulence generating anisotropic heating that drives instabilities?

MMS/FPI Measurements in the Magnetosheath

- *MMS*/FPI burst-mode measurements of protons
  - Burst-mode cadence: 150 ms
  - 58,510 data from 6 distinct intervals
  - Intervals previously studied by Chasapis et al. (*ApJ*, 2017; *ApJL*, 2018)
  - Chosen for duration and turbulence activity
  - Four spacecraft used independently
  - For each interval, $\mathrm{median}(R_p) \approx 1$
- Synchronization of proton and magnetic-field data
- Binning of data over $(\beta_{\parallel p}, R_p)$-plane

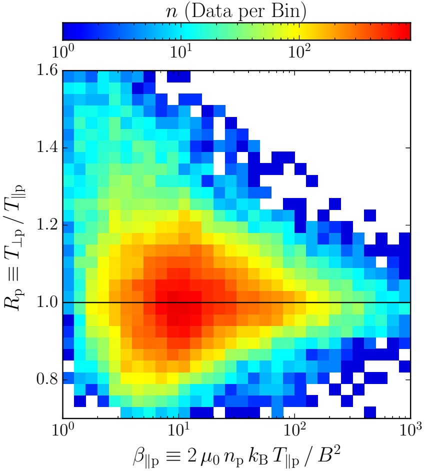

Maruca et al. (*ApJ*, 2018)

Comparison of *MMS* Data and Linear Vlasov Theory

- Same data in both plots
- Low-count bins suppressed
- Normalization by bin size: probability density
- Contours of constant growth rate $\gamma_{\max}$: same code as Maruca et al. (*ApJ*, 2012)
- Very close alignment of data distribution to theoretical contours

Parallel Instabilities

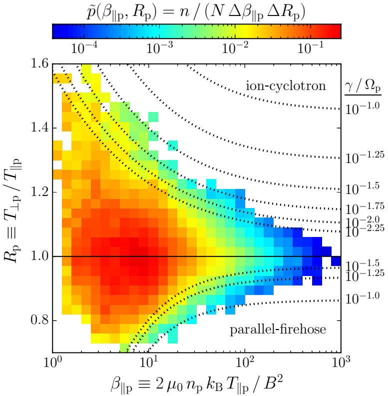

Oblique Instabilities

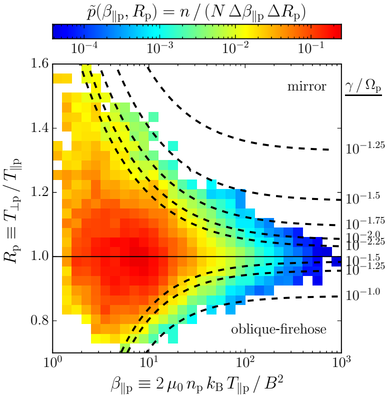

Maruca et al. (*ApJ*, 2018)

Instability Analysis of Time Series

- Multiple, longer periods of *MMS* data
- Growth rates of all 4 ion temperature anisotropy instabilities
- Distinct periods of $\gamma_{\text{max}} > 0$
  - Typical duration $\approx$ few seconds
  - Similar results for parallel and oblique instabilities
  - Some alternation between $R_p < 1$ and $R_p > 1$ periods
- Frequency of $\gamma_{\text{max}} > 0$ periods varies widely

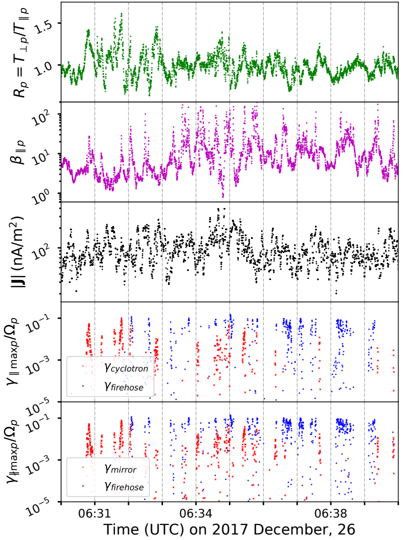

Simulated V Spacecraft Data

- Simulated in-situ observations
  - Choose trajectory and speed through simulation space
  - Generate time series of $\beta_{\|p}$ and R_p values

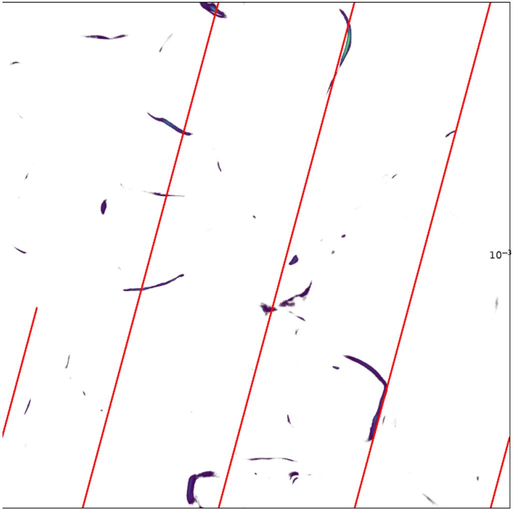

Simulated V Spacecraft Data

- Simulated in-situ observations
  - Choose trajectory and speed through simulation space
  - Generate time series of $\beta_{\parallel p}$ and R_p values
- Upper plot: instability growth rates inferred for $\beta_{\parallel p}$ and R_p values
- Lower plot: growth rates for exemplar period of *MMS* data
- Caveat: computational constraints limited simulation to
  - . . . substantially lower $\beta_{\parallel p}$ than magnetosheath.
  - . . . substantially weaker fluctuations than magnetosheath.

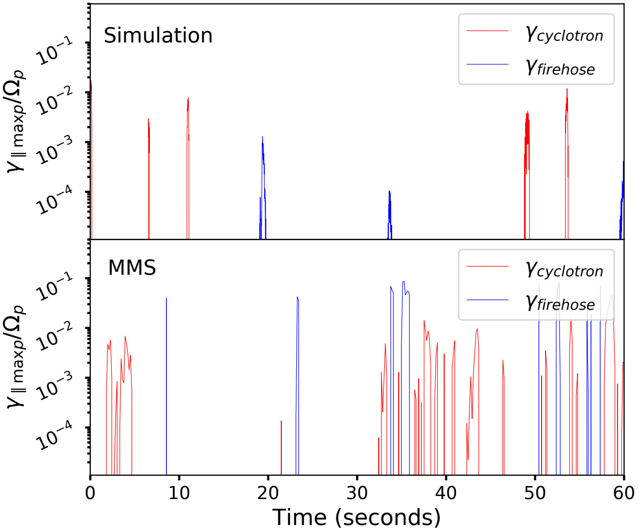

Qudsi et al. (*ApJ*, submitted)

Are these instabilities important?

Majority of solar wind is unstable (∼54 %)

- statistical assessment of solar wind stability at 1 AU against ion sources of free energy using Nyquist's instability criterion
- Considered multiple sources of free energy
- Less than 10% of the spectra have growth rates faster than τ_{nl}

	# Spectra	# Unstable	Mirror	CGL FH	Kinetic
Total	309	166	14	1	151
p, b, & α	189	130	12	0	118
p & α	114	33	2	1	30
p & b	5	3	0	0	3
p	1	0	0	0	0

Klein et al. (*PRL,2018*)

Majority of solar wind is unstable ($\sim$54 %)

- statistical assessment of solar wind stability at 1 AU against ion sources of free energy using Nyquist's instability criterion
- Considered multiple sources of free energy
- Less than 10% of the spectra have growth rates faster than $\tau_{\rm nl}$
  - $\tau_{\rm nl}$ is an estimate for the nonlinear turbulent energy transfer time at the proton gyroscale

	# Spectra	# Unstable	Mirror	CGL FH	Kinetic
Total	309	166	14	1	151
p, b, & α	189	130	12	0	118
p & α	114	33	2	1	30
p & b	5	3	0	0	3
p	1	0	0	0	0

Klein et al. (*PRL,2018*)

$$\tau_{\rm nl} = (k_0\rho_p)^{-1/3}\rho_p/V_A$$

PIC simulation: Comparison between γ and ω

$\tau_{\rm nl}(r) = \ell/\delta b_\ell$

where $\delta b_\ell = |\hat{\boldsymbol{\ell}} \cdot [\mathbf{b}(\mathbf{r} + \boldsymbol{\ell}) - \mathbf{b}(\mathbf{r})]|$

$\omega_{\rm nl} = 2\pi/\tau_{\rm nl}$

PIC simulation: Comparison between γ and ω

$\tau_{\rm nl}(r) = \ell/\delta b_\ell$

where $\delta b_\ell = |\hat{\ell}\cdot[\mathbf{b}(\mathbf{r}+\ell) - \mathbf{b}(\mathbf{r})]|$

$\omega_{\rm nl} = 2\pi/\tau_{\rm nl}$

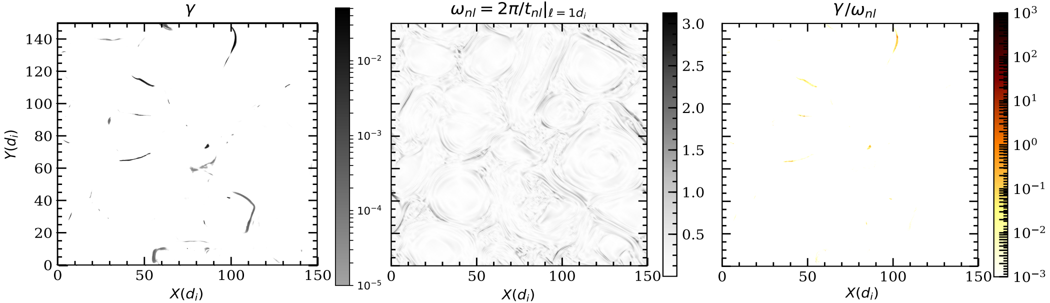

Badyopadhyay et al. (in prep)

Observations: Comparison between γ and ω

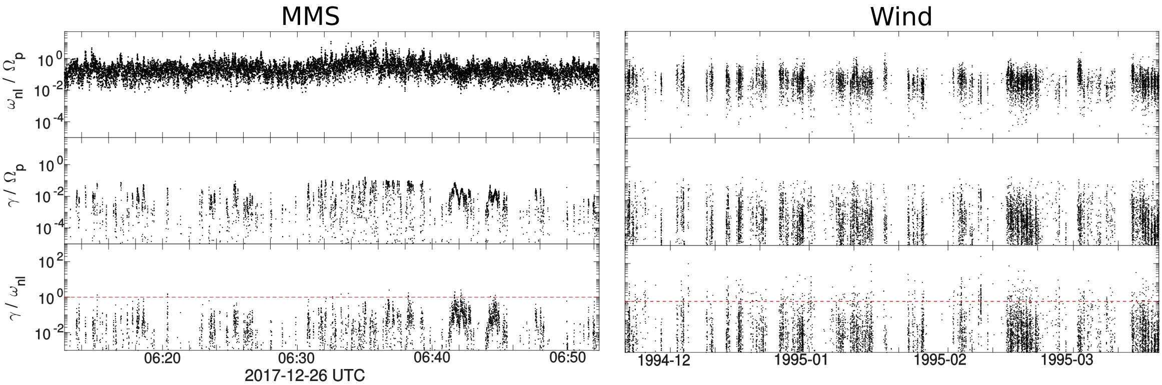

Badyopadhyay et al. (in prep)

Observations: Comparison between γ and ω

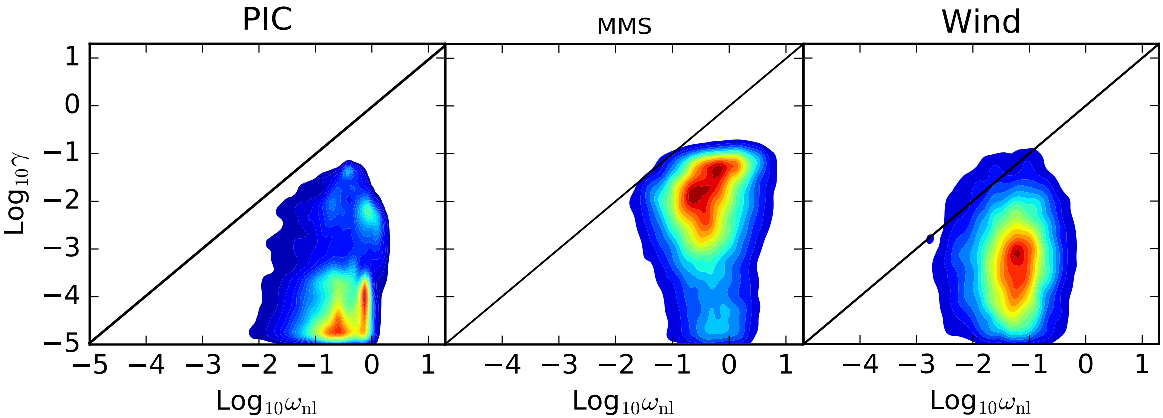

Badyopadhyay et al. (in prep)

Discussion and Conclusions

- Turbulence heats the plasma anisotropically giving rise to anisotropic distribution of instabilities in space plasma

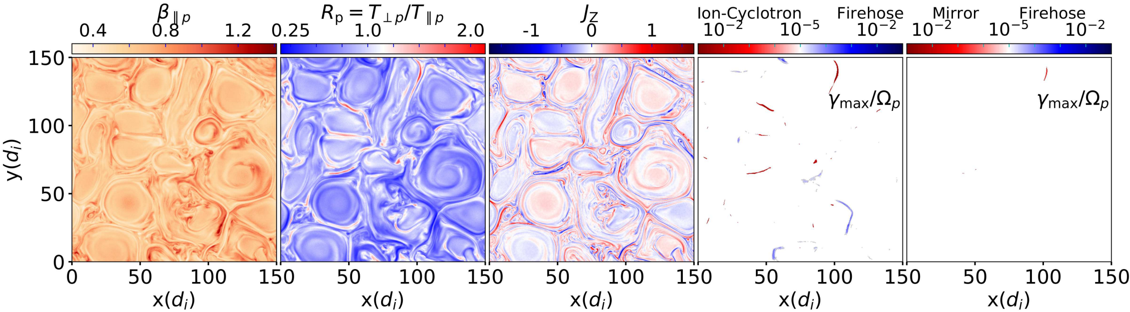

Discussion and Conclusions

- Turbulence heats the plasma anisotropically giving rise to anisotropic distribution of instabilities in space plasma
- The linear instability thresholds acts on plasma and restrict its excursion to extreme values of R_p

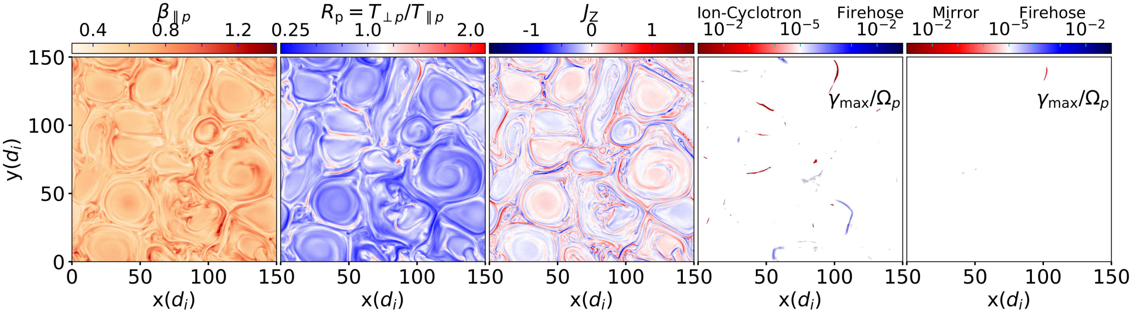

Discussion and Conclusions

- Turbulence heats the plasma anisotropically giving rise to anisotropic distribution of instabilities in space plasma
- The linear instability thresholds acts on plasma and restrict its excursion to extreme values of R_p
- in simulation as well as observational data the non-linear times are almost always faster than the linear time scales

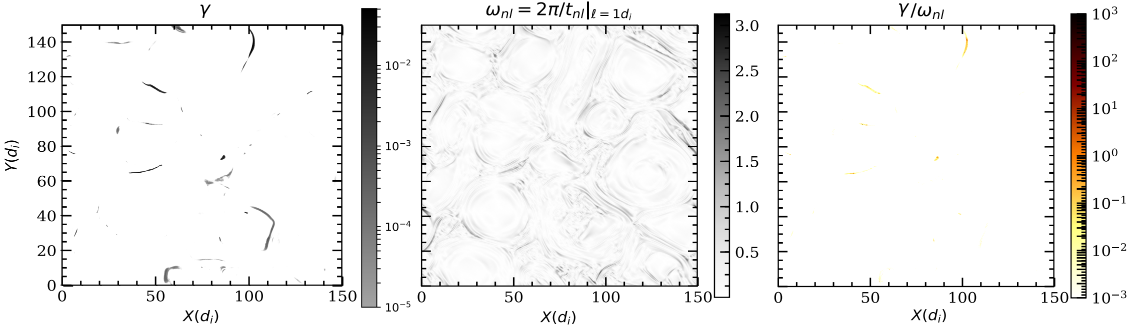

Discussion and Conclusions

- Turbulence heats the plasma anisotropically giving rise to anisotropic distribution of instabilities in space plasma
- The linear instability thresholds acts on plasma and restrict its excursion to extreme values of R_p
- in simulation as well as observational data the non-linear times are almost always faster than the linear time scales

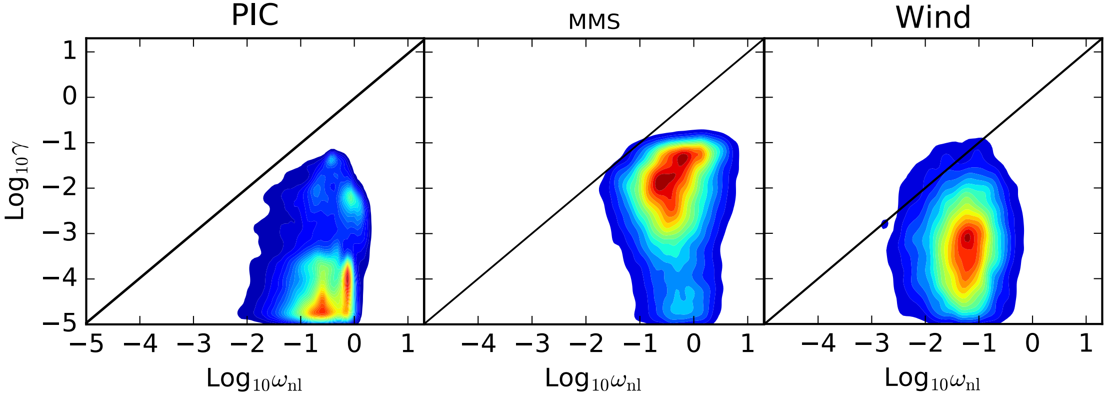

Questions?

Thank you!